



First measurement of the $Z \rightarrow \mu^+ \mu^-$ angular coefficients in the forward region of pp collisions at $\sqrt{s} = 13$ TeV

LHCb collaboration[†]

Abstract

The first study of the angular distribution of $\mu^+ \mu^-$ pairs produced in the forward rapidity region via the Drell-Yan reaction $pp \rightarrow \gamma^*/Z + X \rightarrow \ell^+ \ell^- + X$ is presented, using data collected with the LHCb detector at a center-of-mass energy of 13 TeV, corresponding to an integrated luminosity of 5.1 fb^{-1} . The coefficients of the five leading terms in the angular distribution are determined as a function of the dimuon transverse momentum and rapidity. The results are compared to various theoretical predictions of the Z -boson production mechanism and can also be used to probe transverse-momentum-dependent parton distributions within the proton.

Published in Phys. Rev. Lett. 129 (2022) 091801

© 2022 CERN for the benefit of the LHCb collaboration. CC BY 4.0 licence.

[†]Authors are listed at the end of this Letter.

Drell-Yan muon pairs ($\mu^+\mu^-$) produced near the Z -boson mass pole provide an excellent source of information about electroweak (EW) parameters, probe the proton structure and test the underlying strong-interaction dynamics of Z -boson production in proton-proton (pp) collisions, as described by quantum chromodynamics (QCD). With a dedicated detector instrumented in the forward region, the LHCb experiment plays a unique role in the study of $Z \rightarrow \mu^+\mu^-$ processes in the forward rapidity (y^Z) region [1], especially for $y^Z > 3.5$. Therefore, the LHCb experiment is complementary to the ATLAS and CMS experiments, which are more efficient in the central region. The distributions of the Z -boson transverse momentum, p_T , and the scattering angle, ϕ_η^* , of the muons with respect to the proton beam direction in the rest frame of the dimuon system [2] have already been measured by the LHCb collaboration [1,3–5]. Key information is also encoded in the $Z \rightarrow \mu^+\mu^-$ angular distribution in the forward region, which has not been fully explored.

In the Drell-Yan neutral-current process, the lepton pair is produced via a spin-1 gauge boson. The kinematic distribution of the final-state leptons (ℓ^\pm) provides a direct probe of the polarization of the intermediate gauge boson, which is in turn sensitive to the underlying QCD production mechanisms. The QCD mechanisms of the process $pp \rightarrow \gamma^*/Z + X \rightarrow \ell^+\ell^- + X$, where X represents any other particles, can be expressed using eight frame-dependent angular coefficients, A_i ($i = 0, \dots, 7$). The coefficients depend on the invariant mass, p_T and rapidity of the lepton pair. At Born level, the angular distribution of the leptons in the boson rest frame is given by [6,7]

$$\frac{d\sigma}{d\cos\theta d\phi} \propto (1 + \cos^2\theta) + \frac{1}{2}A_0(1 - 3\cos^2\theta) + A_1\sin 2\theta\cos\phi + \frac{1}{2}A_2\sin^2\theta\cos 2\phi + A_3\sin\theta\cos\phi + A_4\cos\theta + A_5\sin^2\theta\sin 2\phi + A_6\sin 2\theta\sin\phi + A_7\sin\theta\sin\phi, \quad (1)$$

where θ and ϕ are the polar and azimuthal angles of the μ^+ lepton in the Collins-Soper frame [8]. At leading-order (LO) approximation within the framework of QCD, all angular coefficients vanish as the dilepton transverse momentum approaches zero, with the exception of A_4 , which is nonzero due to parity violation in the weak interaction. At next-to-leading-order (NLO), A_{0-3} become nonzero, while A_{5-7} have small deviations from zero only at next-to-next-to-leading-order (NNLO).

The equality $A_0 = A_2$ is known as the Lam-Tung relation [9], which is valid for both $q\bar{q}$ and gq processes at LO [10]. However, small violations of the Lam-Tung relation occur in higher-order perturbative QCD calculations [11,12], as well as in QCD resummation calculations to all orders [13]. Therefore, precision measurements of $A_0 - A_2$ can test the Lam-Tung relation. Nonperturbative effects can lead to violation of the Lam-Tung relation via a correlation between the transverse spin and transverse momentum of the initial-state quark or antiquark, represented by the Boer-Mulders transverse-momentum-dependent (TMD) parton distribution function (PDF) [14,15]. Significant violation of the Lam-Tung relation, with large $\cos 2\phi$ modulations, has been observed in pion-induced Drell-Yan measurements [16–18]. The $\cos 2\phi$ coefficient (A_2) in Eq. (1) is proportional to the convolution of two Boer-Mulders functions, of the quark and the antiquark [15]. Therefore, the angular measurements of the Drell-Yan process can improve constraints on nonperturbative partonic spin-momentum correlations within unpolarised protons via phenomenological extractions of the Boer-Mulders TMD PDF from these data in conjunction with data from other experiments. The Z -boson cross-section measurements

at low p_T ($\lesssim 20$ GeV/ c) by the LHCb collaboration have already been used to extract the unpolarised TMD PDF [19].

Previously, the CDF collaboration published the first measurement [20] of the angular coefficients of lepton pairs produced near the Z -boson mass pole at a hadron collider. Measurements of the W -boson angular coefficients have been published by the CDF [21], CMS [22] and ATLAS [23] collaborations. The CMS collaboration measured A_0 , A_1 , A_2 and A_4 with $Z \rightarrow \mu^+\mu^-$ decays [24], while the ATLAS collaboration reported measurements of the complete set of coefficients [25].

This Letter reports the first measurement of the $Z \rightarrow \mu^+\mu^-$ angular coefficients in the forward rapidity region ($2 < y^Z < 5$) by the LHCb experiment, using Z -boson candidates selected in the mass region $50 < M_{\mu\mu} < 120$ GeV/ c^2 , where $M_{\mu\mu}$ is the invariant mass of the $\mu^+\mu^-$ pair. The parameters A_0 , A_1 , A_2 and A_3 are determined as a function of the Z -boson p_T and y^Z , with the candidates selected in the mass region $75 < M_{\mu\mu} < 105$ GeV/ c^2 . Events in the low mass range, $50 < M_{\mu\mu} < 75$ GeV/ c^2 , and high mass range, $105 < M_{\mu\mu} < 120$ GeV/ c^2 , are used to probe the Boer-Mulders function; these regions are dominated by contributions from virtual photons and their interference with the Z -boson amplitude, with measurements in multiple mass regions adding sensitivity to the evolution of the TMD PDF with the hard scale. With the higher-order QCD effects related to the Z -boson p_T being integrated out, the measurements of the angular coefficients as a function of y^Z can be used to test the resummation calculations in the forward region. Due to the relatively small data sample containing high- p_T (> 50 GeV/ c) $Z \rightarrow \mu^+\mu^-$ events, the coefficients A_5 to A_7 are fixed to zero. Since this study focuses on probing the QCD dynamics of the Z -boson production, the A_4 coefficient, sensitive to the weak mixing angle [26], is not reported. Nevertheless, in order to investigate its variation across the kinematic range, the difference with respect to its mean value, ΔA_4 , is measured.

The LHCb detector [27, 28] is a single-arm forward spectrometer covering the pseudorapidity range $2 < \eta < 5$, designed for the study of particles containing b or c quarks. A silicon-strip vertex detector [29] surrounding the pp interaction region allows c and b hadrons to be identified from their relatively long flight distance. A tracking system [30] provides a measurement of momentum, p , of charged particles, and two imaging Cherenkov detectors [31] are able to discriminate between different species of charged hadrons. Photons, electrons and hadrons are identified by a calorimeter system consisting of scintillating-pad and preshower detectors, an electromagnetic and a hadronic calorimeter. Muons are identified by a system composed of alternating layers of iron and multiwire proportional chambers [32]. The online event selection is performed by a trigger system [33], which consists of a hardware stage, based on information from the calorimeter and muon systems [34, 35], followed by a software stage, which applies a full event reconstruction incorporating near-real-time alignment and calibration of the detector [36].

Simulated pp collisions are generated using PYTHIA8 [37] with a specific LHCb configuration [38]. The interaction of the generated particles with the detector, and its response, are implemented using the GEANT4 toolkit [39] as described in Ref. [40]. Various theoretical predictions at the Born-level are compared with the measured results, including analytic resummed calculations, RESBOS [41] and DYTURBO [42], and a fixed-order calculation with matching algorithms to veto the double counting of quantum electrodynamic (QED) final-state radiation (FSR) and parton shower, POWHEG-BOX [43–46]. Predictions

from the RESBOS [41] generator are produced using the PDF known as CT14HERA2 [47]. The RESBOS calculation combines NLO fixed-order perturbative calculations at high boson p_T , with the soft-gluon Collins-Soper-Sterman resummation formalism [48–50] at low boson p_T , with consideration of a nonperturbative contribution from the parton intrinsic transverse momentum, which is an all-orders summation of large terms from gluon emission. The DYTURBO [42] program is an NNLO generator for the calculation of the QCD transverse-momentum resummation of Drell–Yan cross sections up to next-to-next-to-leading logarithmic accuracy combined with the fixed-order results. DYTURBO includes the full kinematic dependence of the lepton pair with the corresponding spin correlations and finite-width effects. POWHEG-BOX is an NLO generator and can be interfaced with PYTHIA8 for QCD and EW showering, but without the angular damping factors.

Measurements are performed using 5.1 fb^{-1} of data at a center-of-mass energy of 13 TeV collected by the LHCb detector during the years 2016–2018. For each $Z \rightarrow \mu^+ \mu^-$ candidate, at least one of the muons is required to pass hardware and software single-muon trigger decision stages. All muon candidates are required to have transverse momentum $p_T^\mu > 20 \text{ GeV}/c$ and be in the range $2.0 < \eta < 4.5$. The relative uncertainty in the momentum of the muon track must be less than 10%. To further suppress background sources, muon candidates are required to pass an isolation requirement which is parameterised as $z = p_T^\mu / p_T^{\mu\text{-cone}} > 0.85$, where $p_T^{\mu\text{-cone}}$ is the sum of the muon p_T and that of the tracks within $\delta R < 0.5$, and δR is $\sqrt{\delta\eta^2 + \delta\Phi^2}$. The quantities $\delta\eta$ and $\delta\Phi$ give the separation between the muon and neighbouring tracks in pseudorapidity η and the laboratory azimuthal angle Φ , respectively. Candidate Z -bosons are composed of two muon candidates with opposite charge that originate from a common primary pp interaction vertex. In total, 818 074 (745 343) $Z \rightarrow \mu^+ \mu^-$ candidates are selected in the mass region $50 < M_{\mu\mu} < 120 \text{ GeV}/c^2$ ($75 < M_{\mu\mu} < 105 \text{ GeV}/c^2$). Background contributions from heavy-flavour processes and misidentified hadrons are estimated using data control samples [1], while background sources from W^+W^- , $W^\pm Z$, ZZ , $Z \rightarrow \tau^+ \tau^-$ and $t\bar{t}$ processes are estimated from simulation. The total background contribution is determined to be 0.2%.

Detector misalignment effects are studied and suppressed using the $Z \rightarrow \mu^+ \mu^-$ data events, where the mass peak position of the selected Z -boson candidates is calibrated in different kinematic and geometric regions to the world average value [51]. To improve the agreement between data and simulation, selection efficiencies determined from simulation are corrected to corresponding values measured in the data. The selection efficiencies include the muon trigger, muon track reconstruction, muon isolation and identification. These efficiencies are estimated using $Z \rightarrow \mu^+ \mu^-$ data and simulation events, with the tag-and-probe method [1], as functions of muon η and Φ . Additionally, corrections to the momentum scale and resolution are applied to the simulation.

The angular coefficients are determined in six intervals of the Z -boson p_T and five intervals of y^Z , by fitting the two decay angles $\cos\theta$ and ϕ of the selected $Z \rightarrow \mu^+ \mu^-$ candidates, using an unbinned maximum-likelihood method in each interval. The probability density function used in the fit consists of a signal-only function, obtained from Eq. (1), convoluted with the detector resolution and acceptance effects. The angular coefficients (A_{0-4}) are the only free parameters in the fit, while the background contributions are effectively subtracted from the data sample by including background events with negative weights derived from simulation and data control samples. Simulated PYTHIA8 events are

used to study the background modeling along with the detector resolution and acceptance effects, with FSR turned on at the generator level, thereby including the Born/Bare corrections [52]. This way, the measured A_i coefficients are corrected to the Born level. The normalization weights method is used to avoid computing-intensive numerical integration of the probability density function in the fit. This method was introduced and used by the BaBar collaboration [53, 54], and has been extensively used in LHCb heavy-flavour studies [55]. To avoid potential bias from the input angular coefficients in the simulation, an iterative method is used. The measured results are found to be stable after four iterations.

Several sources of systematic uncertainty are considered. Simulation is used to determine the detector acceptance effects in the fit process. To estimate the uncertainty from the finite number of simulated events, the bootstrap method [56] is used. This uncertainty varies from 0.0016 to 0.0402 in different kinematic regions, and is the dominant systematic uncertainty. Another significant uncertainty arises from the selection efficiencies. In the determination of the uncertainty from the efficiency corrections, two independent sources are considered: an uncertainty from the size of the control sample and one from the kinematic dependence of the corrections. For the second uncertainty, the default two-dimensional (muon η and ϕ) efficiency corrections are replaced with one-dimensional corrections, and variations of the results are taken as uncertainties. The fit method is validated with simulation samples. The angular coefficients of the simulation are changed to values far from the default (increased by a factor of 1.5, or set to 0). In the validation, the new angular coefficients are compared with the values from the fit, and differences between them are taken as uncertainties. The uncertainty from the muon momentum scaling and smearing are calculated by varying the corrections by their uncertainties, and the changes in the measured results are taken as the associated systematic uncertainties. These are found to be negligible.

The systematic uncertainties associated to the background are estimated by varying the background contribution by $\pm\sigma$, where σ includes the uncertainties from the theoretical predictions of the cross-sections and the statistical uncertainties from the simulation. The systematic uncertainty from the FSR is estimated by comparing the measured results using the simulation sample weighted to the POWHEG prediction with different FSR algorithms of PHOTOS and PYTHIA8. Differences from different FSR approaches are taken as uncertainties. The systematic uncertainty from the PDF is estimated using 58 sub-PDF sets of CT18NNLO [57], with the prescription recommended by the PDF sets groups [58]. All systematic uncertainties are considered as uncorrelated, and the total systematic uncertainty is taken as their sum in quadrature.

The measured angular coefficients A_{0-3} as well as ΔA_4 and the difference $A_0 - A_2$, are presented as a function of the Z -boson p_T in Fig. 1. The measurements are compared with the predictions of RESBOS, DYTURBO, POWHEG-BOX+PYTHIA8, and PYTHIA8 with LHCb tuning. The measurement of A_0 is in good agreement with DYTURBO, RESBOS, and POWHEG-BOX predictions, but disfavors the PYTHIA8 results in the high p_T region ($> 20 \text{ GeV}/c$). However, the PYTHIA8 calculations show similar increasing trends as the measurements in the high p_T region. The measurement of A_1 disagrees with the PYTHIA8 result, but is in good agreement with other calculations in all p_T regions. Within large statistical uncertainties, the measurements of A_2 are mostly in reasonable agreement with predictions, while for A_3 there is a noticeable underestimation of most predictions up to $55 \text{ GeV}/c^2$. The measured ΔA_4 is in good agreement with theoretical predictions in all

p_T regions. Finally, for the $A_0 - A_2$ measurement, the LHCb results are compatible with zero only in the highest p_T interval, but there the uncertainty is relatively large. Also, most predictions are not compatible with zero in the high- p_T intervals. This violation of the Lam-Tung relations measured by the LHCb collaboration is consistent with previous results from the CMS [24] and ATLAS collaborations [25]. The measured $A_0 - A_2$ results are significantly smaller than the predictions at low p_T (< 20 GeV/ c) and slightly smaller at high p_T (> 80 GeV/ c), while larger than the predictions in other p_T regions. A summary of the full results, including measurements in bins of y^Z , is provided in the Supplemental Material [59]. With the exception of A_0 , the measured angular coefficients do not vary significantly as a function of y^Z , when the measurement is performed for the full p_T range. There is reasonable agreement between the measurements and RESBOS calculations for A_{1-3} and ΔA_4 , while for A_0 there is tension between the measurements and predictions, especially in the highest y^Z region. The p -value between measurements and theoretical predictions is calculated to be 0.06. The differences between A_0 and the RESBOS predictions in the y^Z distribution indicate that there is a y^Z -dependence in the QCD resummation or additional higher-order effects. More detailed studies on the predictions as a function of y^Z are necessary.

The nonperturbative Boer-Mulders TMD PDF can be probed with the measurement of A_2 in the lower p_T region. Measurements of A_2 in the low, middle and high $M_{\mu\mu}$ regions are shown in Fig. 2, where the dimuon p_T region is divided into four intervals from 0–20 GeV/ c . Despite the limited sample size with the finer p_T intervals, several observations can be made. In the low $M_{\mu\mu}$, the measured A_2 value in the lowest dimuon p_T region ($p_T < 3$ GeV/ c) deviates significantly from all predictions. It is unclear if nonperturbative spin-momentum correlations in the proton, described by the Boer-Mulders distribution, could lead to such variations as no phenomenological calculations are available. None of the calculations used in the comparison include this type of nonperturbative effect. In other p_T regions, reasonable agreement between measurements and predictions is seen.

In summary, the first measurements of the angular coefficients of Drell-Yan $\mu^+\mu^-$ pairs in the forward rapidity region of pp collisions are presented. These quantities provide more information on the Z -boson production compared to other traditional observables. The measurements, which are given as a function of the Z -boson p_T and y^Z , in both the Z peak and lower and higher $M_{\mu\mu}$ regions, are compared with various predictions. Some tension between the measurements and the theoretical predictions appears in the lower $M_{\mu\mu}$ and low- p_T region, and in the y^Z dependence (See the Supplemental Material [59] for further details). More studies of the theoretical models are needed to shed light on the apparent discrepancies. This analysis provides important and unique inputs for future phenomenological extractions of spin-momentum correlations in the proton in terms of the Boer-Mulders TMD PDF and its evolution with the hard scale.

Acknowledgements

We express our gratitude to our colleagues in the CERN accelerator departments for the excellent performance of the LHC. We thank the technical and administrative staff at the LHCb institutes. We acknowledge support from CERN and from the national agencies: CAPES, CNPq, FAPERJ and FINEP (Brazil); MOST and NSFC (China); CNRS/IN2P3 (France); BMBF, DFG and MPG (Germany); INFN (Italy); NWO (Netherlands); MNiSW

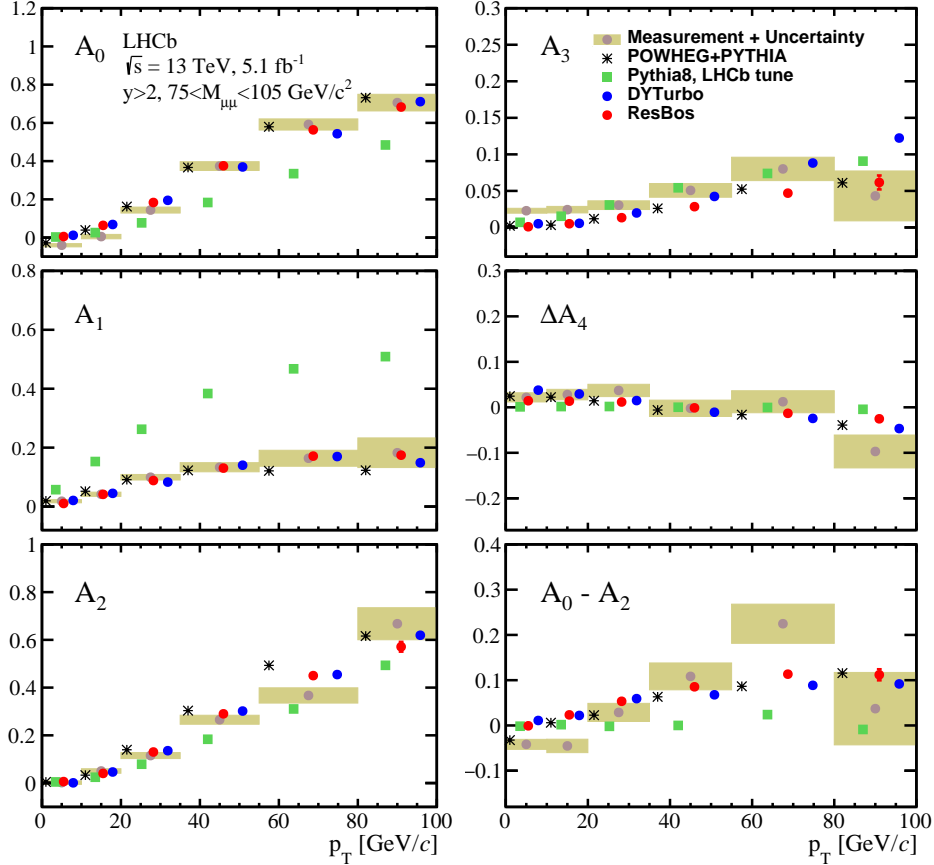


Figure 1: Comparison of the measured angular coefficients with different predictions, as a function of the Z -boson p_T , in the rapidity region of Z -boson $y^Z > 2$ and $75 < M_{\mu\mu} < 105 \text{ GeV}/c^2$. The total uncertainty (shown in the figure) is dominated by the statistical component. The theoretical predictions correspond to the same Z -boson p_T bins as data and the p_T shifts of the theoretical markers in all plots are for visualization purposes only. DYTURBO and RESBOS predictions include the theoretical uncertainties.

and NCN (Poland); MEN/IFA (Romania); MSHE (Russia); MICINN (Spain); SNSF and SER (Switzerland); NASU (Ukraine); STFC (United Kingdom); DOE NP and NSF (USA). We acknowledge the computing resources that are provided by CERN, IN2P3 (France), KIT and DESY (Germany), INFN (Italy), SURF (Netherlands), PIC (Spain), GridPP (United Kingdom), RRCKI and Yandex LLC (Russia), CSCS (Switzerland), IFIN-HH (Romania), CBPF (Brazil), PL-GRID (Poland) and NERSC (USA). We are indebted to the communities behind the multiple open-source software packages on which we depend. Individual groups or members have received support from ARC and ARDC (Australia); AvH Foundation (Germany); EPLANET, Marie Skłodowska-Curie Actions and ERC (European Union); A*MIDEX, ANR, IPhU and Labex P2IO, and Région Auvergne-Rhône-Alpes (France); Key Research Program of Frontier Sciences of CAS, CAS PIFI, CAS CCEPP, Fundamental Research Funds for the Central Universities, and Sci. & Tech. Program of Guangzhou (China); RFBR, RSF and Yandex LLC (Russia); GVA, XuntaGal and GENCAT (Spain); the Leverhulme Trust, the Royal Society and UKRI (United Kingdom).

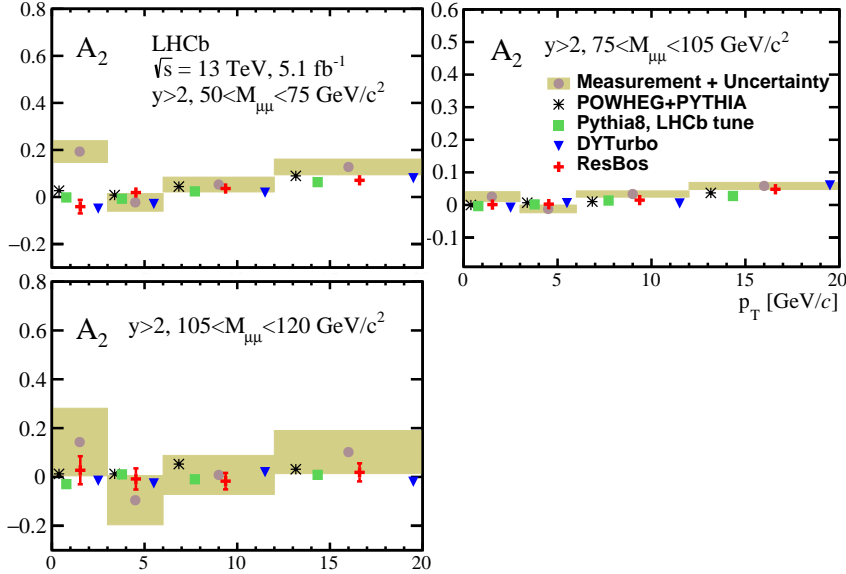


Figure 2: Comparison of the measured angular coefficient A_2 with different predictions, as a function of the Z -boson p_T , in the rapidity region of Z -boson $y^Z > 2$ and $50 < M_{\mu\mu} < 75 \text{ GeV}/c^2$ (left), $50 < M_{\mu\mu} < 75 \text{ GeV}/c^2$ (middle) and $105 < M_{\mu\mu} < 120 \text{ GeV}/c^2$ (right). The total uncertainty (shown in the figure) is dominated by the statistical component. The horizontal positions of the theoretical predictions within the bins are adjusted to increase visibility. DYTURBO and RESBOS predictions include the theoretical uncertainties.

References

- [1] LHCb collaboration, R. Aaij *et al.*, *Precision measurement of forward Z boson production in proton-proton collisions at $\sqrt{s} = 13 \text{ TeV}$* , JHEP **07** (2022) 026, [arXiv:2112.07458](#).
- [2] A. Banfi *et al.*, *Optimisation of variables for studying dilepton transverse momentum distributions at hadron colliders*, Eur. Phys. J. **C71** (2011) 1600, [arXiv:1009.1580](#).
- [3] LHCb collaboration, R. Aaij *et al.*, *Measurement of the forward Z boson cross-section in pp collisions at $\sqrt{s} = 7 \text{ TeV}$* , JHEP **08** (2015) 039, [arXiv:1505.07024](#).
- [4] LHCb collaboration, R. Aaij *et al.*, *Measurement of forward W and Z boson production in pp collisions at $\sqrt{s} = 8 \text{ TeV}$* , JHEP **01** (2016) 155, [arXiv:1511.08039](#).
- [5] LHCb collaboration, R. Aaij *et al.*, *Measurement of the forward Z boson production cross-section in pp collisions at $\sqrt{s} = 13 \text{ TeV}$* , JHEP **09** (2016) 136, [arXiv:1607.06495](#).
- [6] E. Mirkes, J. G. Korner, and G. A. Schuler, *$\mathcal{O}(\alpha_s^2)$ corrections to high q_T polarized gauge boson production at hadron colliders*, Phys. Lett. **B259** (1991) 151.
- [7] J. G. Korner and E. Mirkes, *Polarization density matrix of high q_T gauge bosons in high-energy proton-antiproton collisions*, Nucl. Phys. B Proc. Suppl. **23** (1991) 9.

- [8] J. C. Collins and D. E. Soper, *Angular distribution of dileptons in high-energy hadron collisions*, Phys. Rev. **D16** (1977) 2219.
- [9] C. S. Lam and W.-K. Tung, *Structure function relations at large transverse momenta in lepton-pair production process*, Phys. Lett. **B80** (229) 1979.
- [10] D. Boer and W. Vogelsang, *Drell-Yan lepton angular distribution at small transverse momentum*, Phys. Rev. **D74** (2006) 014004, arXiv:hep-ph/0604177.
- [11] E. Mirkes and J. Ohnemus, *W and Z polarization effects in hadronic collisions*, Phys. Rev. **D50** (1994) 5692, arXiv:hep-ph/9406381.
- [12] R. Gauld *et al.*, *Precise predictions for the angular coefficients in Z-boson production at the LHC*, JHEP **11** (2017) 003, arXiv:1708.00008.
- [13] E. L. Berger, J.-W. Qiu, and R. A. Rodriguez-Pedraza, *Angular distribution of leptons from the decay of massive vector bosons*, Phys. Lett. **B656** (2007) 74, arXiv:0707.3150.
- [14] D. Boer and P. J. Mulders, *Time reversal odd distribution functions in leptonproduction*, Phys. Rev. **D57** (1998) 5780, arXiv:hep-ph/9711485.
- [15] D. Boer, *Investigating the origins of transverse spin asymmetries at RHIC*, Phys. Rev. **D60** (1999) 014012, arXiv:hep-ph/9902255.
- [16] NA10 collaboration, S. Falciano *et al.*, *Angular distributions of muon pairs produced by 194-GeV/c negative pions*, Z. Phys. **C31** (1986) 513.
- [17] NA10 collaboration, M. Guanziroli *et al.*, *Angular distributions of muon pairs produced by negative pions on deuterium and tungsten*, Z. Phys. **C37** (1988) 545.
- [18] J. S. Conway *et al.*, *Experimental study of muon pairs produced by 252-GeV pions on tungsten*, Phys. Rev. **D39** (1989) 92.
- [19] A. Bacchetta *et al.*, *Transverse-momentum-dependent parton distributions up to N^3LL from Drell-Yan data*, JHEP **07** (2020) 117, arXiv:1912.07550.
- [20] CDF collaboration, T. Aaltonen *et al.*, *First measurement of the angular coefficients of Drell-Yan e^+e^- pairs in the Z mass region from $p\bar{p}$ Collisions at $\sqrt{s} = 1.96$ TeV*, Phys. Rev. Lett. **106** (2011) 241801, arXiv:1103.5699.
- [21] CDF collaboration, T. Aaltonen *et al.*, *Measurement of the azimuthal angle distribution of leptons from W boson decays as a function of the W transverse momentum in $p\bar{p}$ collisions at $\sqrt{s} = 1.8$ TeV*, Phys. Rev. **D73** (2006) 052002.
- [22] CMS collaboration, S. Chatrchyan *et al.*, *Measurement of the polarization of W bosons with large transverse momenta in W+Jets events at the LHC*, Phys. Rev. Lett. **107** (2011) 021802, arXiv:1104.3829.
- [23] ATLAS collaboration, G. Aad *et al.*, *Measurement of the polarisation of W bosons produced with large transverse momentum in pp collisions at $\sqrt{s} = 7$ TeV with the ATLAS experiment*, Eur. Phys. J. **C72** (2012) 2001, arXiv:1203.2165.

- [24] CMS collaboration, V. Khachatryan *et al.*, *Angular coefficients of Z bosons produced in pp collisions at $\sqrt{s} = 8$ TeV and decaying to $\mu^+\mu^-$ as a function of transverse momentum and rapidity*, Phys. Lett. **B750** (2015) 154, [arXiv:1504.03512](#).
- [25] ATLAS collaboration, G. Aad *et al.*, *Measurement of the angular coefficients in Z-boson events using electron and muon pairs from data taken at $\sqrt{s} = 8$ TeV with the ATLAS detector*, JHEP **08** (2016) 159, [arXiv:1606.00689](#).
- [26] ALEPH collaboration *et al.*, *Precision electroweak measurements on the Z resonance*, Physics Reports **427** (2006) 257.
- [27] LHCb collaboration, A. A. Alves Jr. *et al.*, *The LHCb detector at the LHC*, JINST **3** (2008) S08005.
- [28] LHCb collaboration, R. Aaij *et al.*, *LHCb detector performance*, Int. J. Mod. Phys. **A30** (2015) 1530022, [arXiv:1412.6352](#).
- [29] R. Aaij *et al.*, *Performance of the LHCb Vertex Locator*, JINST **9** (2014) P09007, [arXiv:1405.7808](#).
- [30] R. Arink *et al.*, *Performance of the LHCb Outer Tracker*, JINST **9** (2014) P01002, [arXiv:1311.3893](#).
- [31] M. Adinolfi *et al.*, *Performance of the LHCb RICH detector at the LHC*, Eur. Phys. J. **C73** (2013) 2431, [arXiv:1211.6759](#).
- [32] A. A. Alves Jr. *et al.*, *Performance of the LHCb muon system*, JINST **8** (2013) P02022, [arXiv:1211.1346](#).
- [33] R. Aaij *et al.*, *The LHCb trigger and its performance in 2011*, JINST **8** (2013) P04022, [arXiv:1211.3055](#).
- [34] C. Abellan Beteta *et al.*, *Calibration and performance of the LHCb calorimeters in Run 1 and 2 at the LHC*, [arXiv:2008.11556](#), submitted to JINST.
- [35] F. Archilli *et al.*, *Performance of the muon identification at LHCb*, JINST **8** (2013) P10020, [arXiv:1306.0249](#).
- [36] G. Dujany and B. Storaci, *Real-time alignment and calibration of the LHCb Detector in Run II*, J. Phys. Conf. Ser. **664** (2015) 082010.
- [37] T. Sjöstrand, S. Mrenna, and P. Skands, *A brief introduction to PYTHIA 8.1*, Comput. Phys. Commun. **178** (2008) 852, [arXiv:0710.3820](#).
- [38] I. Belyaev *et al.*, *Handling of the generation of primary events in Gauss, the LHCb simulation framework*, J. Phys. Conf. Ser. **331** (2011) 032047.
- [39] Geant4 collaboration, J. Allison *et al.*, *Geant4 developments and applications*, IEEE Trans. Nucl. Sci. **53** (2006) 270.
- [40] M. Clemencic *et al.*, *The LHCb simulation application, Gauss: Design, evolution and experience*, J. Phys. Conf. Ser. **331** (2011) 032023.

- [41] C. Balazs and C. P. Yuan, *Soft gluon effects on lepton pairs at hadron colliders*, Phys. Rev. **D56** (1997) 5558, [arXiv:hep-ph/9704258](#).
- [42] S. Camarda *et al.*, *DYTURBO: fast predictions for Drell–Yan processes*, Eur. Phys. J. **C80** (2020) 251, [arXiv:1910.07049](#), [Erratum: Eur.Phys.J.C 80, 440 (2020)].
- [43] P. Nason, *A new method for combining NLO QCD with shower Monte Carlo algorithms*, JHEP **16** (2004) 025.
- [44] S. Frixione, P. Nason, and C. Oleari, *Matching NLO QCD computations with parton shower simulations: the POWHEG method*, J. High Energy Phys **11** (2007) 070, [arXiv:0709.2092](#).
- [45] S. Alioli, P. Nason, C. Oleari, and E. Re, *NLO vector-boson production matched with shower in POWHEG*, J. High Energy Phys **07** (2008) 060, [arXiv:0805.4802](#).
- [46] S. Alioli, P. Nason, C. Oleari, and E. Re, *A general framework for implementing NLO calculations in shower Monte Carlo programs: the POWHEG BOX*, J. High Energy Phys **06** (2010) 043, [arXiv:1002.2581](#).
- [47] T.-J. Hou *et al.*, *CTEQ-TEA parton distribution functions and HERA Run I and II combined data*, Phys. Rev. **D95** (2017) .
- [48] J. C. Collins, D. E. Soper, and G. F. Sterman, *Transverse momentum distribution in Drell-Yan pair and W and Z Boson production*, Nucl. Phys. **B250** (1985) 199.
- [49] J. C. Collins and D. E. Soper, *Back-To-Back jets in QCD*, Nucl. Phys. B **193** (1981) 381, [Erratum: Nucl.Phys.B 213, 545 (1983)].
- [50] J. C. Collins and D. E. Soper, *Back-to-back jets: Fourier transform from b to k_T* , Nucl. Phys. **B197** (1982) 446.
- [51] Particle Data Group, P. A. Zyla *et al.*, *Review of particle physics*, Prog. Theor. Exp. Phys. **2020** (2020) 083C01.
- [52] W. Placzek and S. Jadach, *Multiphoton radiation in leptonic W boson decays*, Eur. Phys. J. **C29** (2003) 325, [arXiv:hep-ph/0302065](#).
- [53] BaBar collaboration, B. Aubert *et al.*, *Measurement of the $B \rightarrow J/\psi K^*(892)$ decay amplitudes*, Phys. Rev. Lett. **87** (2001) 241801, [arXiv:hep-ex/0107049](#).
- [54] BaBar collaboration, B. Aubert *et al.*, *Ambiguity-free measurement of $\cos(2\beta)$: Time-integrated and time-dependent angular analyses of $B \rightarrow J/\psi K\pi$* , Phys. Rev. **D71** (2005) 032005, [arXiv:hep-ex/0411016](#).
- [55] LHCb collaboration, R. Aaij *et al.*, *Measurement of the CP-violating phase ϕ_s in the decay $B_s^0 \rightarrow J/\psi\phi$* , Phys. Rev. Lett. **108** (2012) 101803, [arXiv:1112.3183](#).
- [56] B. Efron, *Bootstrap methods: Another look at the jackknife*, Ann. Statist. **7** (1979) 1.
- [57] T.-J. Hou *et al.*, *New CTEQ global analysis of quantum chromodynamics with high-precision data from the LHC*, Phys. Rev. **D103** (2021) 014013, [arXiv:1912.10053](#).

[58] S. Alekhin *et al.*, *The PDF4LHC Working Group Interim Report*, [arXiv:1101.0536](#).

[59] *See supplemental material*, [publisher to insert link].

Supplemental material

The number of data candidate events in different Z -boson p_T and rapidity intervals are summarized in Table 1. Summaries of measured angular coefficients A_i are shown in Table 2 in intervals of Z -boson p_T , and in Table 3 and Fig. 3 in intervals of Z -boson rapidity. Summaries of measured angular coefficients and regularised uncertainties of A_2 in the Z -boson low- p_T region, with events in different mass regions, are given in Table 4.

Table 1: The number of selected data candidate events in different Z boson p_T and rapidity intervals in the mass region $50 < M_{\mu\mu} < 120 \text{ GeV}/c^2$.

| p_T interval | Yields | y^Z interval | Yields |
|----------------|--------|----------------|--------|
| 0-10 | 366305 | 2-2.7 | 203272 |
| 10-20 | 214341 | 2.7-3 | 171839 |
| 20-35 | 130525 | 3-3.25 | 152349 |
| 35-55 | 63285 | 3.25-3.6 | 171900 |
| 55-80 | 27445 | 3.6-4.5 | 118714 |
| 80-100 | 8120 | | |

Table 2: Summary of measured angular coefficients and regularised uncertainties for A_i and $A_0 - A_2$, in intervals of Z -boson p_T , in the region of Z -boson $y > 2$ and $75 < M_{\mu\mu} < 105 \text{ GeV}/c^2$. The total systematic uncertainty is shown with the breakdown into its underlying components. Entries marked with ‘-’ indicate that the uncertainty is below 0.0001.

| | $p_T(Z) \in [0, 10][\text{GeV}]$ | | | | | | $p_T(Z) \in [10, 20][\text{GeV}]$ | | | | | |
|-------------|-----------------------------------|--------|--------|--------|--------------|-------------|------------------------------------|--------|--------|--------|--------------|-------------|
| Coefficient | A_0 | A_1 | A_2 | A_3 | ΔA_4 | $A_0 - A_2$ | A_0 | A_1 | A_2 | A_3 | ΔA_4 | $A_0 - A_2$ |
| Total | -0.0401 | 0.0180 | 0.0019 | 0.0229 | 0.0219 | -0.0418 | 0.0052 | 0.0417 | 0.0506 | 0.0244 | 0.0280 | -0.0452 |
| Stat | 0.0075 | 0.0046 | 0.0062 | 0.0029 | 0.0054 | 0.0097 | 0.0101 | 0.0061 | 0.0083 | 0.0039 | 0.0073 | 0.0130 |
| Syst | 0.0040 | 0.0028 | 0.0036 | 0.0017 | 0.0030 | 0.0053 | 0.0055 | 0.0037 | 0.0045 | 0.0022 | 0.0042 | 0.0071 |
| MC Stat | 0.0039 | 0.0025 | 0.0033 | 0.0016 | 0.0030 | 0.0051 | 0.0054 | 0.0035 | 0.0044 | 0.0022 | 0.0041 | 0.0070 |
| FSR | - | - | - | - | - | - | - | - | - | - | - | - |
| Eff | - | - | - | - | - | - | - | - | - | - | - | - |
| Bkg | - | - | - | - | - | - | - | - | - | - | - | - |
| Smear | - | - | - | - | - | - | - | - | - | - | - | - |
| PDF | 0.0003 | 0.0003 | 0.0012 | 0.0002 | 0.0001 | 0.0010 | 0.0003 | 0.0004 | 0.0007 | 0.0002 | 0.0006 | 0.0006 |
| Extraction | 0.0008 | 0.0010 | 0.0004 | - | - | 0.0008 | 0.0007 | 0.0013 | 0.0004 | - | 0.0002 | 0.0008 |
| | $p_T(Z) \in [20, 35][\text{GeV}]$ | | | | | | $p_T(Z) \in [35, 55][\text{GeV}]$ | | | | | |
| Coefficient | A_0 | A_1 | A_2 | A_3 | ΔA_4 | $A_0 - A_2$ | A_0 | A_1 | A_2 | A_3 | ΔA_4 | $A_0 - A_2$ |
| Total | 0.1439 | 0.0995 | 0.1152 | 0.0305 | 0.0371 | 0.0288 | 0.3740 | 0.1334 | 0.2653 | 0.0507 | -0.0021 | 0.1084 |
| Stat | 0.0138 | 0.0083 | 0.0110 | 0.0053 | 0.0096 | 0.0176 | 0.0204 | 0.0134 | 0.0166 | 0.0082 | 0.0140 | 0.0263 |
| Syst | 0.0073 | 0.0044 | 0.0061 | 0.0028 | 0.0054 | 0.0095 | 0.0105 | 0.0078 | 0.0090 | 0.0045 | 0.0081 | 0.0138 |
| MC Stat | 0.0071 | 0.0041 | 0.0060 | 0.0027 | 0.0054 | 0.0094 | 0.0104 | 0.0075 | 0.0086 | 0.0044 | 0.0081 | 0.0134 |
| FSR | - | - | - | - | - | - | 0.0003 | 0.0002 | 0.0002 | - | - | 0.0004 |
| Eff | 0.0001 | - | 0.0001 | - | - | 0.0001 | 0.0001 | - | - | - | - | 0.0002 |
| Bkg | - | - | - | - | - | 0.0001 | - | - | - | - | - | - |
| Smear | - | - | - | - | - | - | - | - | - | - | - | - |
| PDF | 0.0009 | 0.0009 | 0.0007 | 0.0002 | 0.0003 | 0.0014 | 0.0006 | 0.0004 | 0.0023 | 0.0009 | 0.0003 | 0.0019 |
| Extraction | 0.0010 | 0.0014 | 0.0006 | 0.0001 | 0.0001 | 0.0012 | 0.0016 | 0.0021 | 0.0017 | 0.0005 | 0.0005 | 0.0023 |
| | $p_T(Z) \in [55, 80][\text{GeV}]$ | | | | | | $p_T(Z) \in [80, 100][\text{GeV}]$ | | | | | |
| Coefficient | A_0 | A_1 | A_2 | A_3 | ΔA_4 | $A_0 - A_2$ | A_0 | A_1 | A_2 | A_3 | ΔA_4 | $A_0 - A_2$ |
| Total | 0.5917 | 0.1639 | 0.3671 | 0.0801 | 0.0123 | 0.2247 | 0.7061 | 0.1826 | 0.6676 | 0.0432 | -0.0971 | 0.0371 |
| Stat | 0.0261 | 0.0237 | 0.0275 | 0.0139 | 0.0200 | 0.0379 | 0.0378 | 0.0442 | 0.0572 | 0.0293 | 0.0311 | 0.0686 |
| Syst | 0.0130 | 0.0132 | 0.0163 | 0.0079 | 0.0110 | 0.0209 | 0.0217 | 0.0241 | 0.0351 | 0.0175 | 0.0167 | 0.0413 |
| MC Stat | 0.0121 | 0.0129 | 0.0160 | 0.0079 | 0.0110 | 0.0201 | 0.0206 | 0.0233 | 0.0345 | 0.0174 | 0.0165 | 0.0402 |
| FSR | 0.0006 | 0.0001 | 0.0004 | - | 0.0001 | 0.0008 | 0.0004 | 0.0008 | 0.0005 | 0.0002 | - | 0.0006 |
| Eff | 0.0006 | 0.0002 | 0.0003 | 0.0001 | 0.0002 | 0.0007 | 0.0004 | 0.0004 | 0.0008 | 0.0005 | 0.0002 | 0.0009 |
| Bkg | 0.0002 | 0.0001 | 0.0002 | - | 0.0001 | 0.0003 | 0.0005 | 0.0002 | 0.0008 | 0.0002 | 0.0002 | 0.0009 |
| Smear | - | - | - | - | - | - | - | - | - | - | - | - |
| PDF | 0.0010 | 0.0017 | 0.0009 | 0.0006 | 0.0008 | 0.0016 | 0.0011 | 0.0024 | 0.0041 | 0.0009 | 0.0015 | 0.0035 |
| Extraction | 0.0045 | 0.0021 | 0.0029 | 0.0008 | 0.0004 | 0.0054 | 0.0067 | 0.0056 | 0.0054 | 0.0010 | 0.0019 | 0.0086 |

Table 3: Summary of measured angular coefficients and regularised uncertainties for A_i and $A_0 - A_2$, in intervals of Z -boson rapidity, in the region of Z -boson $p_T < 100 \text{ GeV}/c$ and $75 < M_{\mu\mu} < 105 \text{ GeV}/c^2$. The total systematic uncertainty is shown with the breakdown into its underlying components. Entries marked with ‘-’ indicate that the uncertainty is below 0.0001.

| | $y^Z \in [2, 2.7]$ | | | | | | $y^Z \in [2.7, 3]$ | | | | | |
|-------------|---------------------|--------|--------|--------|--------------|-------------|-----------------------|--------|--------|--------|--------------|-------------|
| Coefficient | A_0 | A_1 | A_2 | A_3 | ΔA_4 | $A_0 - A_2$ | A_0 | A_1 | A_2 | A_3 | ΔA_4 | $A_0 - A_2$ |
| Total | 0.1124 | 0.0354 | 0.0958 | 0.0357 | -0.0321 | 0.0162 | 0.0543 | 0.0659 | 0.0843 | 0.0388 | 0.0026 | -0.0302 |
| Stat | 0.0180 | 0.0085 | 0.0078 | 0.0039 | 0.0103 | 0.0197 | 0.0119 | 0.0067 | 0.0096 | 0.0046 | 0.0077 | 0.0153 |
| Syst | 0.0102 | 0.0046 | 0.0044 | 0.0022 | 0.0062 | 0.0112 | 0.0068 | 0.0038 | 0.0055 | 0.0024 | 0.0041 | 0.0088 |
| MC Stat | 0.0102 | 0.0044 | 0.0043 | 0.0022 | 0.0062 | 0.0111 | 0.0067 | 0.0035 | 0.0054 | 0.0024 | 0.0041 | 0.0086 |
| FSR | 0.0006 | 0.0013 | 0.0004 | 0.0001 | 0.0001 | 0.0007 | 0.0006 | 0.0013 | 0.0005 | 0.0002 | - | 0.0008 |
| Eff | 0.0005 | 0.0002 | 0.0001 | - | - | 0.0005 | 0.0002 | - | - | - | - | 0.0002 |
| Bkg | 0.0003 | - | 0.0001 | - | - | 0.0003 | 0.0001 | - | - | - | - | 0.0001 |
| Smear | - | - | - | - | - | - | - | - | - | - | - | - |
| PDF | 0.0001 | 0.0003 | 0.0004 | 0.0001 | 0.0004 | 0.0004 | 0.0007 | 0.0010 | 0.0011 | 0.0003 | 0.0004 | 0.0017 |
| Extraction | 0.0011 | 0.0002 | 0.0004 | - | 0.0004 | 0.0012 | 0.0006 | 0.0001 | 0.0003 | 0.0001 | 0.0003 | 0.0007 |
| | $y^Z \in [3, 3.25]$ | | | | | | $y^Z \in [3.25, 3.6]$ | | | | | |
| Coefficient | A_0 | A_1 | A_2 | A_3 | ΔA_4 | $A_0 - A_2$ | A_0 | A_1 | A_2 | A_3 | ΔA_4 | $A_0 - A_2$ |
| Total | 0.0708 | 0.0665 | 0.0778 | 0.0144 | 0.0029 | -0.0070 | 0.0443 | 0.0723 | 0.0583 | 0.0341 | 0.0171 | -0.0139 |
| Stat | 0.0107 | 0.0068 | 0.0110 | 0.0051 | 0.0075 | 0.0154 | 0.0102 | 0.0065 | 0.0102 | 0.0047 | 0.0072 | 0.0145 |
| Syst | 0.0058 | 0.0039 | 0.0064 | 0.0028 | 0.0040 | 0.0087 | 0.0053 | 0.0036 | 0.0059 | 0.0026 | 0.0037 | 0.0078 |
| MC Stat | 0.0057 | 0.0036 | 0.0063 | 0.0027 | 0.0040 | 0.0085 | 0.0052 | 0.0031 | 0.0057 | 0.0026 | 0.0037 | 0.0077 |
| FSR | 0.0009 | 0.0015 | 0.0007 | 0.0003 | - | 0.0012 | 0.0007 | 0.0015 | 0.0006 | 0.0002 | - | 0.0010 |
| Eff | 0.0001 | - | 0.0001 | - | - | 0.0002 | 0.0001 | - | - | - | - | 0.0002 |
| Bkg | - | - | 0.0001 | - | - | 0.0002 | - | - | - | - | - | - |
| Smear | - | - | - | - | - | - | - | - | - | - | - | - |
| PDF | 0.0005 | 0.0004 | 0.0006 | 0.0006 | 0.0004 | 0.0009 | 0.0006 | 0.0008 | 0.0008 | 0.0004 | 0.0003 | 0.0005 |
| Extraction | 0.0002 | 0.0001 | 0.0007 | - | 0.0002 | 0.0007 | 0.0004 | 0.0001 | 0.0006 | 0.0001 | 0.0002 | 0.0007 |

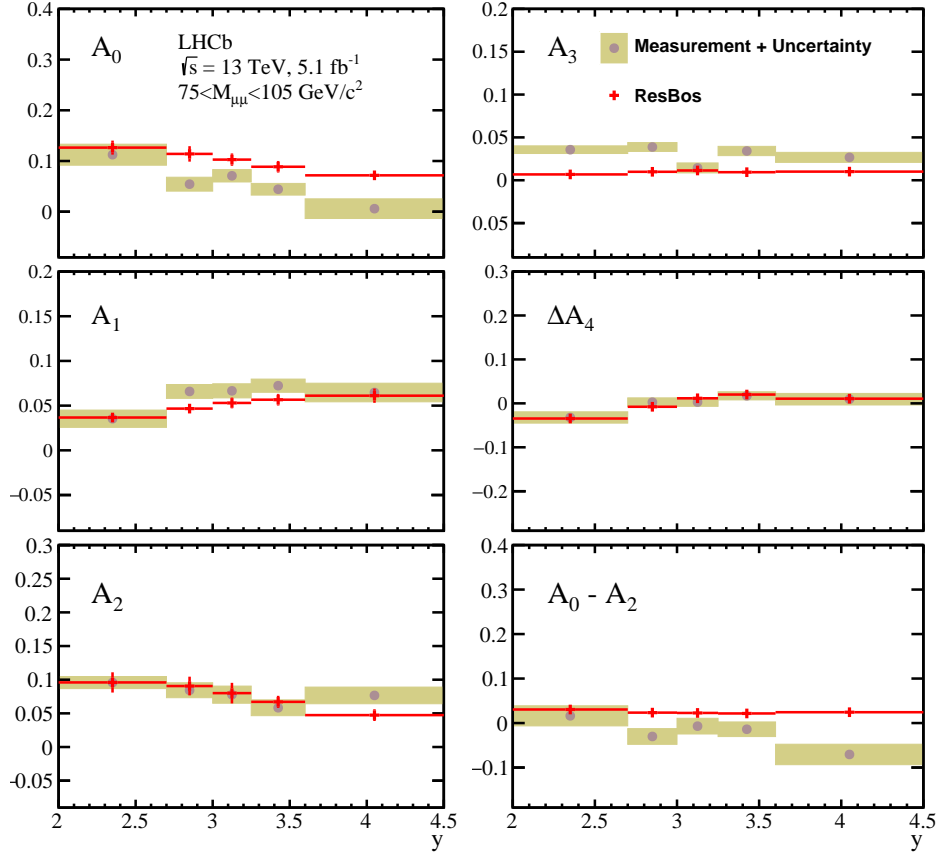


Figure 3: Comparison of the measured angular coefficients with RESBOS predictions as a function of the y^Z in the $75 < M_{\mu\mu} < 105 \text{ GeV}/c^2$ mass region. The total uncertainty (shown in the figure) is dominated by the statistical component. RESBOS predictions include the theoretical uncertainties.

Table 4: Summary of measured angular coefficients and regularised uncertainties for A_2 , in intervals of Z -boson p_T , in the region of Z -boson $y > 2$ and different mass ranges. The total systematic uncertainty is shown with the breakdown into its underlying components. Entries marked with ‘-’ indicate that the uncertainty is below 0.0001.

| $p_T(Z) \in [0, 3][\text{GeV}]$ | | | |
|-----------------------------------|-------------------------------------------|--------------------------------------------|---------------------------------------------|
| | $M_{\mu\mu} \in [55, 75] \text{ GeV}/c^2$ | $M_{\mu\mu} \in [75, 105] \text{ GeV}/c^2$ | $M_{\mu\mu} \in [105, 120] \text{ GeV}/c^2$ |
| Coefficient | A_2 | A_2 | A_2 |
| Total | 0.1931 | 0.0255 | 0.1429 |
| Stat | 0.0399 | 0.0132 | 0.1204 |
| Syst | 0.0235 | 0.0077 | 0.0685 |
| MC Stat | 0.0230 | 0.0075 | 0.0680 |
| FSR | 0.0007 | - | 0.0008 |
| Eff | 0.0012 | 0.0002 | 0.0022 |
| Bkg | 0.0012 | - | 0.0013 |
| Smear | - | - | - |
| PDF | 0.0028 | 0.0017 | 0.0079 |
| Extraction | 0.0032 | 0.0002 | 0.0017 |
| $p_T(Z) \in [3, 6][\text{GeV}]$ | | | |
| | $M_{\mu\mu} \in [55, 75] \text{ GeV}/c^2$ | $M_{\mu\mu} \in [75, 105] \text{ GeV}/c^2$ | $M_{\mu\mu} \in [105, 120] \text{ GeV}/c^2$ |
| Coefficient | A_2 | A_2 | A_2 |
| Total | -0.0230 | -0.0122 | -0.0952 |
| Stat | 0.0323 | 0.0102 | 0.0883 |
| Syst | 0.0191 | 0.0062 | 0.0485 |
| MC Stat | 0.0177 | 0.0060 | 0.0483 |
| FSR | 0.0009 | - | 0.0002 |
| Eff | 0.0007 | - | 0.0013 |
| Bkg | 0.0007 | - | 0.0005 |
| Smear | - | - | - |
| PDF | 0.0062 | 0.0013 | 0.0044 |
| Extraction | 0.0033 | 0.0006 | 0.0028 |
| $p_T(Z) \in [6, 12][\text{GeV}]$ | | | |
| | $M_{\mu\mu} \in [55, 75] \text{ GeV}/c^2$ | $M_{\mu\mu} \in [75, 105] \text{ GeV}/c^2$ | $M_{\mu\mu} \in [105, 120] \text{ GeV}/c^2$ |
| Coefficient | A_2 | A_2 | A_2 |
| Total | 0.0530 | 0.0335 | 0.0083 |
| Stat | 0.0274 | 0.0083 | 0.0692 |
| Syst | 0.0157 | 0.0048 | 0.0398 |
| MC Stat | 0.0152 | 0.0046 | 0.0390 |
| FSR | 0.0002 | - | 0.0012 |
| Eff | 0.0006 | - | 0.0017 |
| Bkg | 0.0002 | - | 0.0019 |
| Smear | - | - | - |
| PDF | 0.0019 | 0.0011 | 0.0072 |
| Extraction | 0.0029 | 0.0005 | 0.0019 |
| $p_T(Z) \in [12, 20][\text{GeV}]$ | | | |
| | $M_{\mu\mu} \in [55, 75] \text{ GeV}/c^2$ | $M_{\mu\mu} \in [75, 105] \text{ GeV}/c^2$ | $M_{\mu\mu} \in [105, 120] \text{ GeV}/c^2$ |
| Coefficient | A_2 | A_2 | A_2 |
| Total | 0.1278 | 0.0583 | 0.1018 |
| Stat | 0.0291 | 0.0097 | 0.0760 |
| Syst | 0.0167 | 0.0052 | 0.0449 |
| MC Stat | 0.0164 | 0.0049 | 0.0422 |
| FSR | 0.0006 | 0.0002 | 0.0013 |
| Eff | 0.0009 | - | 0.0014 |
| Bkg | 0.0007 | 0.0001 | 0.0005 |
| Smear | - | - | - |
| PDF | 0.0028 | 0.0010 | 0.0151 |
| Extraction | 0.0013 | 0.0012 | 0.0028 |

LHCb collaboration

R. Aaij³², A.S.W. Abdelmotteleb⁵⁶, C. Abellán Beteta⁵⁰, F. Abudinén⁵⁶, T. Ackernley⁶⁰,
 B. Adeva⁴⁶, M. Adinolfi⁵⁴, H. Afsharnia⁹, C. Agapopoulou¹³, C.A. Aidala⁸⁶, S. Aiola²⁵,
 Z. Ajaltouni⁹, S. Akar⁶⁵, J. Albrecht¹⁵, F. Alessio⁴⁸, M. Alexander⁵⁹, A. Alfonso Alberio⁴⁵,
 Z. Aliouche⁶², G. Alkhazov³⁸, P. Alvarez Cartelle⁵⁵, S. Amato², J.L. Amey⁵⁴, Y. Amhis^{11,48},
 L. An⁴⁸, L. Anderlini²², M. Andersson⁵⁰, A. Andreianov³⁸, M. Andreotti²¹, D. Andreou⁶⁸,
 D. Ao⁶, F. Archilli¹⁷, A. Artamonov⁴⁴, M. Artuso⁶⁸, E. Aslanides¹⁰, M. Atzeni⁵⁰, B. Audurier¹²,
 S. Bachmann¹⁷, M. Bachmayer⁴⁹, J.J. Back⁵⁶, P. Baladron Rodriguez⁴⁶, V. Balagura¹²,
 W. Baldini²¹, J. Baptista de Souza Leite¹, M. Barbetti^{22,h}, R.J. Barlow⁶², S. Barsuk¹¹,
 W. Barter⁶¹, M. Bartolini⁵⁵, F. Baryshnikov⁸², J.M. Basels¹⁴, G. Bassi²⁹, B. Batsukh⁴,
 A. Battig¹⁵, A. Bay⁴⁹, A. Beck⁵⁶, M. Becker¹⁵, F. Bedeschi²⁹, I. Bediaga¹, A. Beiter⁶⁸,
 V. Belavin⁴², S. Belin⁴⁶, V. Bellee⁵⁰, K. Belous⁴⁴, I. Belov⁴⁰, I. Belyaev⁴¹, G. Bencivenni²³,
 E. Ben-Haim¹³, A. Berezhnoy⁴⁰, R. Bernet⁵⁰, D. Berninghoff¹⁷, H.C. Bernstein⁶⁸, C. Bertella⁶²,
 A. Bertolin²⁸, C. Betancourt⁵⁰, F. Betti⁴⁸, Ia. Bezshyiko⁵⁰, S. Bhasin⁵⁴, J. Bhom³⁵, L. Bian⁷³,
 M.S. Bieker¹⁵, N.V. Biesuz²¹, S. Bifani⁵³, P. Billoir¹³, A. Biolchini³², M. Birch⁶¹,
 F.C.R. Bishop⁵⁵, A. Bitadze⁶², A. Bizzeti^{22,l}, M.P. Blago⁵⁵, T. Blake⁵⁶, F. Blanc⁴⁹, S. Blusk⁶⁸,
 D. Bobulska⁵⁹, J.A. Boelhaue¹⁵, O. Boente Garcia⁴⁶, T. Boettcher⁶⁵, A. Boldyrev⁸¹,
 A. Bondar⁴³, N. Bondar^{38,48}, S. Borghi⁶², M. Borsato¹⁷, J.T. Borsuk³⁵, S.A. Bouchiba⁴⁹,
 T.J.V. Bowcock^{60,48}, A. Boyer⁴⁸, C. Bozzi²¹, M.J. Bradley⁶¹, S. Braun⁶⁶, A. Brea Rodriguez⁴⁶,
 J. Brodzicka³⁵, A. Brossa Gonzalo⁵⁶, D. Brundu²⁷, A. Buonaura⁵⁰, L. Buonincontri²⁸,
 A.T. Burke⁶², C. Burr⁴⁸, A. Bursche⁷², A. Butkevich³⁹, J.S. Butter³², J. Buytaert⁴⁸,
 W. Byczynski⁴⁸, S. Cadeddu²⁷, H. Cai⁷³, R. Calabrese^{21,g}, L. Calefice^{15,13}, S. Cali²³,
 R. Calladine⁵³, M. Calvi^{26,k}, M. Calvo Gomez⁸⁴, P. Camargo Magalhaes⁵⁴, P. Campana²³,
 D.H. Campora Perez⁷⁹, A.F. Campoverde Quezada⁶, S. Capelli^{26,k}, L. Capriotti^{20,e},
 A. Carbone^{20,e}, G. Carboni^{31,q}, R. Cardinale^{24,i}, A. Cardini²⁷, I. Carli⁴, P. Carniti^{26,k},
 L. Carus¹⁴, K. Carvalho Akiba³², A. Casais Vidal⁴⁶, R. Caspary¹⁷, G. Casse⁶⁰, M. Cattaneo⁴⁸,
 G. Cavallero⁴⁸, S. Celani⁴⁹, J. Cerasoli¹⁰, D. Cervenkov⁶³, A.J. Chadwick⁶⁰, M.G. Chapman⁵⁴,
 M. Charles¹³, Ph. Charpentier⁴⁸, C.A. Chavez Barajas⁶⁰, M. Chefdeville⁸, C. Chen³, S. Chen⁴,
 A. Chernov³⁵, S. Chernyshenko⁵², V. Chobanova⁴⁶, S. Cholak⁴⁹, M. Chrzaszcz³⁵,
 A. Chubykin³⁸, V. Chulikov³⁸, P. Ciambrone²³, M.F. Cicala⁵⁶, X. Cid Vidal⁴⁶, G. Ciezarek⁴⁸,
 P.E.L. Clarke⁵⁸, M. Clemencic⁴⁸, H.V. Cliff⁵⁵, J. Closier⁴⁸, J.L. Cobbedick⁶², V. Coco⁴⁸,
 J.A.B. Coelho¹¹, J. Cogan¹⁰, E. Cogneras⁹, L. Cojocariu³⁷, P. Collins⁴⁸, T. Colombo⁴⁸,
 L. Congedo¹⁹, A. Contu²⁷, N. Cooke⁵³, G. Coombs⁵⁹, I. Corredoira⁴⁶, G. Corti⁴⁸,
 B. Couturier⁴⁸, D.C. Craik⁶⁴, J. Crkovačka⁶⁷, M. Cruz Torres¹, R. Currie⁵⁸, C.L. Da Silva⁶⁷,
 S. Dadabaev⁸², L. Dai⁷¹, E. Dall’Occo¹⁵, J. Dalseno⁴⁶, C. D’Ambrosio⁴⁸, A. Danilina⁴¹,
 P. d’Argent¹⁵, A. Dashkina⁸², J.E. Davies⁶², A. Davis⁶², O. De Aguiar Francisco⁶²,
 J. De Boer⁴⁸, K. De Bruyn⁷⁸, S. De Capua⁶², M. De Cian⁴⁹, U. De Freitas Carneiro Da Graca¹,
 E. De Lucia²³, J.M. De Miranda¹, L. De Paula², M. De Serio^{19,d}, D. De Simone⁵⁰,
 P. De Simone²³, F. De Vellis¹⁵, J.A. de Vries⁷⁹, C.T. Dean⁶⁷, F. Debernardis^{19,d}, D. Decamp⁸,
 V. Dedu¹⁰, L. Del Buono¹³, B. Delaney⁵⁵, H.-P. Dembinski¹⁵, V. Denysenko⁵⁰, D. Derkach⁸¹,
 O. Deschamps⁹, F. Dettori²⁷, B. Dey⁷⁶, A. Di Cicco²³, P. Di Nezza²³, S. Didenko⁸²,
 L. Dieste Maronas⁴⁶, S. Ding⁶⁸, V. Dobishuk⁵², A. Dolmatov⁸², C. Dong³, A.M. Donohoe¹⁸,
 F. Dordei²⁷, A.C. dos Reis¹, L. Douglas⁵⁹, A.G. Downes⁸, M.W. Dudek³⁵, L. Dufour⁴⁸,
 V. Duk⁷⁷, P. Durante⁴⁸, J.M. Durham⁶⁷, D. Dutta⁶², A. Dziurda³⁵, A. Dzyuba³⁸, S. Easo⁵⁷,
 U. Egede⁶⁹, V. Egorychev⁴¹, S. Eidelman^{43,u,†}, S. Eisenhardt⁵⁸, S. Ek-In⁴⁹, L. Eklund⁸⁵,
 S. Ely⁶⁸, A. Ene³⁷, E. Epple⁶⁷, S. Escher¹⁴, J. Eschle⁵⁰, S. Esen⁵⁰, T. Evans⁶², L.N. Falcao¹,
 Y. Fan⁶, B. Fang⁷³, S. Farry⁶⁰, D. Fazzini^{26,k}, M. Féo⁴⁸, A.D. Fernez⁶⁶, F. Ferrari²⁰,
 L. Ferreira Lopes⁴⁹, F. Ferreira Rodrigues², S. Ferreres Sole³², M. Ferrillo⁵⁰, M. Ferro-Luzzi⁴⁸,
 S. Filippov³⁹, R.A. Fini¹⁹, M. Fiorini^{21,g}, M. Firlej³⁴, K.M. Fischer⁶³, D.S. Fitzgerald⁸⁶,

C. Fitzpatrick⁶², T. Fiutowski³⁴, A. Fkiaras⁴⁸, F. Fleuret¹², M. Fontana¹³, F. Fontanelli^{24,i},
 R. Forty⁴⁸, D. Foulds-Holt⁵⁵, V. Franco Lima⁶⁰, M. Franco Sevilla⁶⁶, M. Frank⁴⁸, E. Franzoso²¹,
 G. Frau¹⁷, C. Frei⁴⁸, D.A. Friday⁵⁹, J. Fu⁶, Q. Fuehring¹⁵, E. Gabriel³², G. Galati^{19,d},
 A. Gallas Torreira⁴⁶, D. Galli^{20,e}, S. Gambetta^{58,48}, Y. Gan³, M. Gandelman², P. Gandini²⁵,
 Y. Gao⁵, M. Garau²⁷, L.M. Garcia Martin⁵⁶, P. Garcia Moreno⁴⁵, J. García Pardiñas^{26,k},
 B. Garcia Plana⁴⁶, F.A. Garcia Rosales¹², L. Garrido⁴⁵, C. Gaspar⁴⁸, R.E. Geertsema³²,
 D. Gerick¹⁷, L.L. Gerken¹⁵, E. Gersabeck⁶², M. Gersabeck⁶², T. Gershon⁵⁶, L. Giambastiani²⁸,
 V. Gibson⁵⁵, H.K. Giemza³⁶, A.L. Gilman⁶³, M. Giovannetti^{23,q}, A. Gioventù⁴⁶,
 P. Gironella Gironell⁴⁵, C. Giugliano²¹, M.A. Giza³⁵, K. Gizdov⁵⁸, E.L. Gkougkousis⁴⁸,
 V.V. Gligorov^{13,48}, C. Göbel⁷⁰, E. Golobardes⁸⁴, D. Golubkov⁴¹, A. Golutvin^{61,82}, A. Gomes^{1,a},
 S. Gomez Fernandez⁴⁵, F. Goncalves Abrantes⁶³, M. Goncerz³⁵, G. Gong³, P. Gorbounov⁴¹,
 I.V. Gorelov⁴⁰, C. Gotti²⁶, J.P. Grabowski¹⁷, T. Grammatico¹³, L.A. Granado Cardoso⁴⁸,
 E. Graugés⁴⁵, E. Graverini⁴⁹, G. Graziani²², A. Greco³⁷, L.M. Greeven³², N.A. Grieser⁴,
 L. Grillo⁶², S. Gromov⁸², B.R. Gruberg Cazon⁶³, C. Gu³, M. Guarise²¹, M. Guittiere¹¹, P.
 A. Günther¹⁷, E. Gushchin³⁹, A. Guth¹⁴, Y. Guz⁴⁴, T. Gys⁴⁸, T. Hadavizadeh⁶⁹, G. Haefeli⁴⁹,
 C. Haen⁴⁸, J. Haimberger⁴⁸, S.C. Haines⁵⁵, T. Halewood-leagas⁶⁰, M.M. Halvorsen⁴⁸,
 P.M. Hamilton⁶⁶, J.P. Hammerich⁶⁰, Q. Han⁷, X. Han¹⁷, E.B. Hansen⁶²,
 S. Hansmann-Menzemer^{17,48}, N. Harnew⁶³, T. Harrison⁶⁰, C. Hasse⁴⁸, M. Hatch⁴⁸, J. He^{6,b},
 K. Heijhoff³², K. Heinicke¹⁵, R.D.L. Henderson^{69,56}, A.M. Hennequin⁶⁴, K. Hennessy⁶⁰,
 L. Henry⁴⁸, J. Heuel¹⁴, A. Hicheur², D. Hill⁴⁹, M. Hilton⁶², S.E. Hollitt¹⁵, R. Hou⁷, Y. Hou⁸,
 J. Hu¹⁷, J. Hu⁷², W. Hu⁵, X. Hu³, W. Huang⁶, X. Huang⁷³, W. Hulsbergen³², R.J. Hunter⁵⁶,
 M. Hushchyn⁸¹, D. Hutchcroft⁶⁰, P. Ibis¹⁵, M. Idzik³⁴, D. Ilin³⁸, P. Ilten⁶⁵, A. Inglessi³⁸,
 A. Iniukhin⁸¹, A. Ishteev⁸², K. Ivshin³⁸, R. Jacobsson⁴⁸, H. Jage¹⁴, S. Jakobsen⁴⁸, E. Jans³²,
 B.K. Jashal⁴⁷, A. Jawahery⁶⁶, V. Jevtic¹⁵, X. Jiang⁴, M. John⁶³, D. Johnson⁶⁴, C.R. Jones⁵⁵,
 T.P. Jones⁵⁶, B. Jost⁴⁸, N. Jurik⁴⁸, I. Juszczak³⁵, S. Kandybei⁵¹, Y. Kang³, M. Karacson⁴⁸,
 D. Karpenkov⁸², M. Karpov⁸¹, J.W. Kautz⁶⁵, F. Keizer⁴⁸, D.M. Keller⁶⁸, M. Kenzie⁵⁶,
 T. Ketel³³, B. Khanji¹⁵, A. Kharisova⁸³, S. Kholodenko^{44,82}, T. Kirn¹⁴, V.S. Kirsebom⁴⁹,
 O. Kitouni⁶⁴, S. Klaver³³, N. Kleijne²⁹, K. Klimaszewski³⁶, M.R. Kmiec³⁶, S. Koliiev⁵²,
 A. Kondybayeva⁸², A. Konoplyannikov⁴¹, P. Kopciewicz³⁴, R. Kopecna¹⁷, P. Koppenburg³²,
 M. Korolev⁴⁰, I. Kostiuk^{32,52}, O. Kot⁵², S. Kotriakhova^{21,38}, A. Kozachuk⁴⁰, P. Kravchenko³⁸,
 L. Kravchuk³⁹, R.D. Krawczyk⁴⁸, M. Kreps⁵⁶, S. Kretzschmar¹⁴, P. Krokovny^{43,u}, W. Krupa³⁴,
 W. Krzemien³⁶, J. Kubat¹⁷, M. Kucharczyk³⁵, V. Kudryavtsev^{43,u}, G.J. Kunde⁶⁷,
 D. Lacarrere⁴⁸, G. Lafferty⁶², A. Lai²⁷, A. Lampis²⁷, D. Lancierini⁵⁰, J.J. Lane⁶², R. Lane⁵⁴,
 G. Lanfranchi²³, C. Langenbruch¹⁴, J. Langer¹⁵, O. Lantwin⁸², T. Latham⁵⁶, F. Lazzari²⁹,
 R. Le Gac¹⁰, S.H. Lee⁸⁶, R. Lefèvre⁹, A. Leflat⁴⁰, S. Legotin⁸², O. Leroy¹⁰, T. Lesiak³⁵,
 B. Leverington¹⁷, H. Li⁷², K. Li⁷, P. Li¹⁷, S. Li⁷, Y. Li⁴, Z. Li⁶⁸, X. Liang⁶⁸, C. Lin⁶, T. Lin⁵⁷,
 R. Lindner⁴⁸, V. Lisovskyi¹⁵, R. Litvinov²⁷, G. Liu⁷², H. Liu⁶, Q. Liu⁶, S. Liu⁴,
 A. Lobo Salvia⁴⁵, A. Loi²⁷, R. Lollini⁷⁷, J. Lomba Castro⁴⁶, I. Longstaff⁵⁹, J.H. Lopes²,
 S. López Soliño⁴⁶, G.H. Lovell⁵⁵, Y. Lu⁴, C. Lucarelli^{22,h}, D. Lucchesi^{28,m}, S. Luchuk³⁹,
 M. Lucio Martinez³², V. Lukashenko^{32,52}, Y. Luo³, A. Lupato⁶², E. Luppi^{21,g}, A. Lusiani^{29,n},
 K. Lynch¹⁸, X. Lyu⁶, L. Ma⁴, R. Ma⁶, S. Maccolini²⁰, F. Machefer¹¹, F. Maciuc³⁷, V. Macko⁴⁹,
 P. Mackowiak¹⁵, S. Maddrell-Mander⁵⁴, L.R. Madhan Mohan⁵⁴, O. Maev³⁸, A. Maevskiy⁸¹,
 D. Maisuzenko³⁸, M.W. Majewski³⁴, J.J. Malczewski³⁵, S. Malde⁶³, B. Malecki³⁵, A. Malinin⁸⁰,
 T. Maltsev^{43,u}, H. Malygina¹⁷, G. Manca^{27,f}, G. Mancinelli¹⁰, D. Manuzzi²⁰, C.A. Manzari⁵⁰,
 D. Marangotto^{25,j}, J. Maratas^{9,s}, J.F. Marchand⁸, U. Marconi²⁰, S. Mariani^{22,h},
 C. Marin Benito⁴⁵, M. Marinangeli⁴⁹, J. Marks¹⁷, A.M. Marshall⁵⁴, P.J. Marshall⁶⁰,
 G. Martelli⁷⁷, G. Martellotti³⁰, L. Martinazzoli^{48,k}, M. Martinelli^{26,k}, D. Martinez Santos⁴⁶,
 F. Martinez Vidal⁴⁷, A. Massafferri¹, M. Materok¹⁴, R. Matev⁴⁸, A. Mathad⁵⁰, V. Matiunin⁴¹,
 C. Matteuzzi²⁶, K.R. Mattioli⁸⁶, A. Mauri³², E. Maurice¹², J. Mauricio⁴⁵, M. Mazurek⁴⁸,
 M. McCann⁶¹, L. McConnell¹⁸, T.H. Mcgrath⁶², N.T. Mchugh⁵⁹, A. McNab⁶², R. McNulty¹⁸,

J.V. Mead⁶⁰, B. Meadows⁶⁵, G. Meier¹⁵, D. Melnychuk³⁶, S. Meloni^{26,k}, M. Merk^{32,79},
 A. Merli^{25,j}, L. Meyer Garcia², M. Mikhasenko^{75,c}, D.A. Milanes⁷⁴, E. Millard⁵⁶,
 M. Milovanovic⁴⁸, M.-N. Minard⁸, A. Minotti^{26,k}, S.E. Mitchell⁵⁸, B. Mitreska⁶², D.S. Mitzel¹⁵,
 A. Mödden¹⁵, R.A. Mohammed⁶³, R.D. Moise⁶¹, S. Mokhnenko⁸¹, T. Mombächer⁴⁶,
 I.A. Monroy⁷⁴, S. Monteil⁹, M. Morandin²⁸, G. Morello²³, M.J. Morello^{29,n}, J. Moron³⁴,
 A.B. Morris⁷⁵, A.G. Morris⁵⁶, R. Mountain⁶⁸, H. Mu³, F. Muheim⁵⁸, M. Mulder⁷⁸, K. Müller⁵⁰,
 C.H. Murphy⁶³, D. Murray⁶², R. Murta⁶¹, P. Muzzetto²⁷, P. Naik⁵⁴, T. Nakada⁴⁹,
 R. Nandakumar⁵⁷, T. Nanut⁴⁸, I. Nasteva², M. Needham⁵⁸, N. Neri^{25,j}, S. Neubert⁷⁵,
 N. Neufeld⁴⁸, R. Newcombe⁶¹, E.M. Niel⁴⁹, S. Nieswand¹⁴, N. Nikitin⁴⁰, N.S. Nolte⁶⁴,
 C. Normand⁸, C. Nunez⁸⁶, A. Oblakowska-Mucha³⁴, V. Obraztsov⁴⁴, T. Oeser¹⁴,
 D.P. O'Hanlon⁵⁴, S. Okamura²¹, R. Oldeman^{27,f}, F. Oliva⁵⁸, M.E. Olivares⁶⁸,
 C.J.G. Onderwater⁷⁸, R.H. O'Neil⁵⁸, J.M. Otalora Goicochea², T. Ovsiannikova⁴¹, P. Owen⁵⁰,
 A. Oyanguren⁴⁷, O. Ozcelik⁵⁸, K.O. Padeken⁷⁵, B. Pagare⁵⁶, P.R. Pais⁴⁸, T. Pajero⁶³,
 A. Palano¹⁹, M. Palutan²³, Y. Pan⁶², G. Panshin⁸³, A. Papanestis⁵⁷, M. Pappagallo^{19,d},
 L.L. Pappalardo²¹, C. Pappenheimer⁶⁵, W. Parker⁶⁶, C. Parkes⁶², B. Passalacqua²¹,
 G. Passaleva²², A. Pastore¹⁹, M. Patel⁶¹, C. Patrignani^{20,e}, C.J. Pawley⁷⁹, A. Pearce^{48,57},
 A. Pellegrino³², M. Pepe Altarelli⁴⁸, S. Perazzini²⁰, D. Pereima⁴¹, A. Pereiro Castro⁴⁶,
 P. Perret⁹, M. Petric^{59,48}, K. Petridis⁵⁴, A. Petrolini^{24,i}, A. Petrov⁸⁰, S. Petrucci⁵⁸,
 M. Petruzzo²⁵, T.T.H. Pham⁶⁸, A. Philippov⁴², R. Piandani⁶, L. Pica^{29,n},
 E. Picatoste Olloqui⁴⁵, M. Piccini⁷⁷, B. Pietrzyk⁸, G. Pietrzyk¹¹, M. Pili⁶³, D. Pinci³⁰,
 F. Pisani⁴⁸, M. Pizzichemi^{26,48,k}, Resmi P.K¹⁰, V. Placinta³⁷, J. Plews⁵³, M. Plo Casasus⁴⁶,
 F. Polci^{13,48}, M. Poli Lener²³, M. Poliakova⁶⁸, A. Poluektov¹⁰, N. Polukhina^{82,t}, I. Polyakov⁶⁸,
 E. Polycarpo², S. Ponce⁴⁸, D. Popov^{6,48}, S. Popov⁴², S. Poslavskii⁴⁴, K. Prasanth³⁵,
 L. Promberger⁴⁸, C. Prouve⁴⁶, V. Pugatch⁵², V. Puill¹¹, G. Punzi^{29,o}, H. Qi³, W. Qian⁶,
 N. Qin³, S. Qu³, R. Quagliani⁴⁹, N.V. Raab¹⁸, R.I. Rabadan Trejo⁶, B. Rachwal³⁴,
 J.H. Rademacker⁵⁴, R. Rajagopalan⁶⁸, M. Rama²⁹, M. Ramos Pernas⁵⁶, M.S. Rangel²,
 F. Ratnikov^{42,81}, G. Raven^{33,48}, M. Rebollo De Miguel⁴⁷, F. Redi⁴⁸, F. Reiss⁶²,
 C. Remon Alepuz⁴⁷, Z. Ren³, V. Renaudin⁶³, R. Ribatti²⁹, A.M. Ricci²⁷, S. Ricciardi⁵⁷,
 K. Rinnert⁶⁰, P. Robbe¹¹, G. Robertson⁵⁸, A.B. Rodrigues⁴⁹, E. Rodrigues⁶⁰,
 J.A. Rodriguez Lopez⁷⁴, E.R.R. Rodriguez Rodriguez⁴⁶, A. Rollings⁶³, P. Roloff⁴⁸,
 V. Romanovskiy⁴⁴, M. Romero Lamas⁴⁶, A. Romero Vidal⁴⁶, J.D. Roth^{86,†}, M. Rotondo²³,
 M.S. Rudolph⁶⁸, T. Ruf⁴⁸, R.A. Ruiz Fernandez⁴⁶, J. Ruiz Vidal⁴⁷, A. Ryzhikov⁸¹, J. Ryzka³⁴,
 J.J. Saborido Silva⁴⁶, N. Sagidova³⁸, N. Sahoo⁵³, B. Saitta^{27,f}, M. Salomoni⁴⁸,
 C. Sanchez Gras³², I. Sanderswood⁴⁷, R. Santacesaria³⁰, C. Santamarina Rios⁴⁶,
 M. Santimaria²³, E. Santovetti^{31,q}, D. Saranin⁸², G. Sarpis¹⁴, M. Sarpis⁷⁵, A. Sarti³⁰,
 C. Satriano^{30,p}, A. Satta³¹, M. Saur¹⁵, D. Savrina^{41,40}, H. Sazak⁹, L.G. Scantlebury Smead⁶³,
 A. Scarabotto¹³, S. Schael¹⁴, S. Scherl⁶⁰, M. Schiller⁵⁹, H. Schindler⁴⁸, M. Schmelling¹⁶,
 B. Schmidt⁴⁸, S. Schmitt¹⁴, O. Schneider⁴⁹, A. Schopper⁴⁸, M. Schubiger³², S. Schulte⁴⁹,
 M.H. Schune¹¹, R. Schwemmer⁴⁸, B. Sciascia^{23,48}, S. Sellam⁴⁶, A. Semennikov⁴¹,
 M. Senghi Soares³³, A. Sergi^{24,i}, N. Serra⁵⁰, L. Sestini²⁸, A. Seuthe¹⁵, Y. Shang⁵,
 D.M. Shangase⁸⁶, M. Shapkin⁴⁴, I. Shchemerov⁸², L. Shchutska⁴⁹, T. Shears⁶⁰,
 L. Shekhtman^{43,u}, Z. Shen⁵, S. Sheng⁴, V. Shevchenko⁸⁰, E.B. Shields^{26,k}, Y. Shimizu¹¹,
 E. Shmanin⁸², J.D. Shupperd⁶⁸, B.G. Siddi²¹, R. Silva Coutinho⁵⁰, G. Simi²⁸, S. Simone^{19,d},
 M. Singla⁶⁹, N. Skidmore⁶², R. Skuza¹⁷, T. Skwarnicki⁶⁸, M.W. Slater⁵³, I. Slazyk^{21,g},
 J.C. Smallwood⁶³, J.G. Smeaton⁵⁵, E. Smith⁵⁰, M. Smith⁶¹, A. Snoch³², L. Soares Lavra⁹,
 M.D. Sokoloff⁶⁵, F.J.P. Soler⁵⁹, A. Solovev³⁸, I. Solovyev³⁸, F.L. Souza De Almeida²,
 B. Souza De Paula², B. Spaan^{15,†}, E. Spadaro Norella^{25,j}, P. Spradlin⁵⁹, V. Sriskaran⁴⁸,
 F. Stagni⁴⁸, M. Stahl⁶⁵, S. Stahl⁴⁸, S. Stanislaus⁶³, O. Steinkamp^{50,82}, O. Stenyakin⁴⁴,
 H. Stevens¹⁵, S. Stone^{68,48,†}, D. Strekalina⁸², F. Suljik⁶³, J. Sun²⁷, L. Sun⁷³, Y. Sun⁶⁶,
 P. Svihra⁶², P.N. Swallow⁵³, K. Swientek³⁴, A. Szabelski³⁶, T. Szumlak³⁴, M. Szymanski⁴⁸,

S. Taneja⁶², A.R. Tanner⁵⁴, M.D. Tat⁶³, A. Terentev⁸², F. Teubert⁴⁸, E. Thomas⁴⁸,
D.J.D. Thompson⁵³, K.A. Thomson⁶⁰, H. Tilquin⁶¹, V. Tisserand⁹, S. T'Jampens⁸, M. Tobin⁴,
L. Tomassetti^{21,g}, G. Tonani²⁵, X. Tong⁵, D. Torres Machado¹, D.Y. Tou³, E. Trifonova⁸²,
S.M. Trilov⁵⁴, C. Tripl⁴⁹, G. Tuci⁶, A. Tully⁴⁹, N. Tuning^{32,48}, A. Ukleja³⁶, D.J. Unverzagt¹⁷,
E. Ursov⁸², A. Usachov³², A. Ustyuzhanin^{42,81}, U. Uwer¹⁷, A. Vagner⁸³, V. Vagnoni²⁰,
A. Valassi⁴⁸, G. Valenti²⁰, N. Valls Canudas⁸⁴, M. van Beuzekom³², M. Van Dijk⁴⁹,
H. Van Hecke⁶⁷, E. van Herwijnen⁸², M. van Veghel⁷⁸, R. Vazquez Gomez⁴⁵,
P. Vazquez Regueiro⁴⁶, C. Vázquez Sierra⁴⁸, S. Vecchi²¹, J.J. Velthuis⁵⁴, M. Veltri^{22,r},
A. Venkateswaran⁶⁸, M. Veronesi³², M. Vesterinen⁵⁶, D. Vieira⁶⁵, M. Vieites Diaz⁴⁹,
X. Vilasis-Cardona⁸⁴, E. Vilella Figueras⁶⁰, A. Villa²⁰, P. Vincent¹³, F.C. Volle¹¹,
D. Vom Bruch¹⁰, A. Vorobyev³⁸, V. Vorobyev^{43,u}, N. Voropaev³⁸, K. Vos⁷⁹, R. Waldi¹⁷,
J. Walsh²⁹, C. Wang¹⁷, J. Wang⁵, J. Wang⁴, J. Wang³, J. Wang⁷³, M. Wang⁵, R. Wang⁵⁴,
Y. Wang⁷, Z. Wang⁵⁰, Z. Wang³, Z. Wang⁶, J.A. Ward^{56,69}, N.K. Watson⁵³, D. Websdale⁶¹,
C. Weisser⁶⁴, B.D.C. Westhenry⁵⁴, D.J. White⁶², M. Whitehead⁵⁴, A.R. Wiederhold⁵⁶,
D. Wiedner¹⁵, G. Wilkinson⁶³, M. K. Wilkinson⁶⁵, I. Williams⁵⁵, M. Williams⁶⁴,
M.R.J. Williams⁵⁸, R. Williams⁵⁵, F.F. Wilson⁵⁷, W. Wislicki³⁶, M. Witek³⁵, L. Witola¹⁷,
C.P. Wong⁶⁷, G. Wormser¹¹, S.A. Wotton⁵⁵, H. Wu⁶⁸, K. Wyllie⁴⁸, Z. Xiang⁶, D. Xiao⁷,
Y. Xie⁷, A. Xu⁵, J. Xu⁶, L. Xu³, M. Xu⁵⁶, Q. Xu⁶, Z. Xu⁹, Z. Xu⁶, D. Yang³, S. Yang⁶,
Y. Yang⁶, Z. Yang⁵, Z. Yang⁶⁶, L.E. Yeomans⁶⁰, H. Yin⁷, J. Yu⁷¹, X. Yuan⁶⁸, O. Yushchenko⁴⁴,
E. Zaffaroni⁴⁹, M. Zavertyaev^{16,t}, M. Zdybal³⁵, O. Zenaiev⁴⁸, M. Zeng³, D. Zhang⁷, L. Zhang³,
S. Zhang⁷¹, S. Zhang⁵, Y. Zhang⁵, Y. Zhang⁶³, A. Zharkova⁸², A. Zhelezov¹⁷, Y. Zheng⁶,
T. Zhou⁵, X. Zhou⁶, Y. Zhou⁶, V. Zhovkovska¹¹, X. Zhu³, X. Zhu⁷, Z. Zhu⁶, V. Zhukov^{14,40},
Q. Zou⁴, S. Zucchelli^{20,e}, D. Zuliani²⁸, G. Zunica⁶².

¹Centro Brasileiro de Pesquisas Físicas (CBPF), Rio de Janeiro, Brazil

²Universidade Federal do Rio de Janeiro (UFRJ), Rio de Janeiro, Brazil

³Center for High Energy Physics, Tsinghua University, Beijing, China

⁴Institute Of High Energy Physics (IHEP), Beijing, China

⁵School of Physics State Key Laboratory of Nuclear Physics and Technology, Peking University, Beijing, China

⁶University of Chinese Academy of Sciences, Beijing, China

⁷Institute of Particle Physics, Central China Normal University, Wuhan, Hubei, China

⁸Univ. Savoie Mont Blanc, CNRS, IN2P3-LAPP, Annecy, France

⁹Université Clermont Auvergne, CNRS/IN2P3, LPC, Clermont-Ferrand, France

¹⁰Aix Marseille Univ, CNRS/IN2P3, CPPM, Marseille, France

¹¹Université Paris-Saclay, CNRS/IN2P3, IJCLab, Orsay, France

¹²Laboratoire Leprince-Ringuet, CNRS/IN2P3, Ecole Polytechnique, Institut Polytechnique de Paris, Palaiseau, France

¹³LPNHE, Sorbonne Université, Paris Diderot Sorbonne Paris Cité, CNRS/IN2P3, Paris, France

¹⁴I. Physikalisches Institut, RWTH Aachen University, Aachen, Germany

¹⁵Fakultät Physik, Technische Universität Dortmund, Dortmund, Germany

¹⁶Max-Planck-Institut für Kernphysik (MPIK), Heidelberg, Germany

¹⁷Physikalisches Institut, Ruprecht-Karls-Universität Heidelberg, Heidelberg, Germany

¹⁸School of Physics, University College Dublin, Dublin, Ireland

¹⁹INFN Sezione di Bari, Bari, Italy

²⁰INFN Sezione di Bologna, Bologna, Italy

²¹INFN Sezione di Ferrara, Ferrara, Italy

²²INFN Sezione di Firenze, Firenze, Italy

²³INFN Laboratori Nazionali di Frascati, Frascati, Italy

²⁴INFN Sezione di Genova, Genova, Italy

²⁵INFN Sezione di Milano, Milano, Italy

²⁶INFN Sezione di Milano-Bicocca, Milano, Italy

²⁷INFN Sezione di Cagliari, Monserrato, Italy

²⁸Università degli Studi di Padova, Università e INFN, Padova, Padova, Italy

- ²⁹ *INFN Sezione di Pisa, Pisa, Italy*
- ³⁰ *INFN Sezione di Roma La Sapienza, Roma, Italy*
- ³¹ *INFN Sezione di Roma Tor Vergata, Roma, Italy*
- ³² *Nikhef National Institute for Subatomic Physics, Amsterdam, Netherlands*
- ³³ *Nikhef National Institute for Subatomic Physics and VU University Amsterdam, Amsterdam, Netherlands*
- ³⁴ *AGH - University of Science and Technology, Faculty of Physics and Applied Computer Science, Kraków, Poland*
- ³⁵ *Henryk Niewodniczanski Institute of Nuclear Physics Polish Academy of Sciences, Kraków, Poland*
- ³⁶ *National Center for Nuclear Research (NCBJ), Warsaw, Poland*
- ³⁷ *Horia Hulubei National Institute of Physics and Nuclear Engineering, Bucharest-Magurele, Romania*
- ³⁸ *Petersburg Nuclear Physics Institute NRC Kurchatov Institute (PNPI NRC KI), Gatchina, Russia*
- ³⁹ *Institute for Nuclear Research of the Russian Academy of Sciences (INR RAS), Moscow, Russia*
- ⁴⁰ *Institute of Nuclear Physics, Moscow State University (SINP MSU), Moscow, Russia*
- ⁴¹ *Institute of Theoretical and Experimental Physics NRC Kurchatov Institute (ITEP NRC KI), Moscow, Russia*
- ⁴² *Yandex School of Data Analysis, Moscow, Russia*
- ⁴³ *Budker Institute of Nuclear Physics (SB RAS), Novosibirsk, Russia*
- ⁴⁴ *Institute for High Energy Physics NRC Kurchatov Institute (IHEP NRC KI), Protvino, Russia, Protvino, Russia*
- ⁴⁵ *ICCUB, Universitat de Barcelona, Barcelona, Spain*
- ⁴⁶ *Instituto Galego de Física de Altas Enerxías (IGFAE), Universidade de Santiago de Compostela, Santiago de Compostela, Spain*
- ⁴⁷ *Instituto de Física Corpuscular, Centro Mixto Universidad de Valencia - CSIC, Valencia, Spain*
- ⁴⁸ *European Organization for Nuclear Research (CERN), Geneva, Switzerland*
- ⁴⁹ *Institute of Physics, Ecole Polytechnique Fédérale de Lausanne (EPFL), Lausanne, Switzerland*
- ⁵⁰ *Physik-Institut, Universität Zürich, Zürich, Switzerland*
- ⁵¹ *NSC Kharkiv Institute of Physics and Technology (NSC KIPT), Kharkiv, Ukraine*
- ⁵² *Institute for Nuclear Research of the National Academy of Sciences (KINR), Kyiv, Ukraine*
- ⁵³ *University of Birmingham, Birmingham, United Kingdom*
- ⁵⁴ *H.H. Wills Physics Laboratory, University of Bristol, Bristol, United Kingdom*
- ⁵⁵ *Cavendish Laboratory, University of Cambridge, Cambridge, United Kingdom*
- ⁵⁶ *Department of Physics, University of Warwick, Coventry, United Kingdom*
- ⁵⁷ *STFC Rutherford Appleton Laboratory, Didcot, United Kingdom*
- ⁵⁸ *School of Physics and Astronomy, University of Edinburgh, Edinburgh, United Kingdom*
- ⁵⁹ *School of Physics and Astronomy, University of Glasgow, Glasgow, United Kingdom*
- ⁶⁰ *Oliver Lodge Laboratory, University of Liverpool, Liverpool, United Kingdom*
- ⁶¹ *Imperial College London, London, United Kingdom*
- ⁶² *Department of Physics and Astronomy, University of Manchester, Manchester, United Kingdom*
- ⁶³ *Department of Physics, University of Oxford, Oxford, United Kingdom*
- ⁶⁴ *Massachusetts Institute of Technology, Cambridge, MA, United States*
- ⁶⁵ *University of Cincinnati, Cincinnati, OH, United States*
- ⁶⁶ *University of Maryland, College Park, MD, United States*
- ⁶⁷ *Los Alamos National Laboratory (LANL), Los Alamos, United States*
- ⁶⁸ *Syracuse University, Syracuse, NY, United States*
- ⁶⁹ *School of Physics and Astronomy, Monash University, Melbourne, Australia, associated to ⁵⁶*
- ⁷⁰ *Pontifícia Universidade Católica do Rio de Janeiro (PUC-Rio), Rio de Janeiro, Brazil, associated to ²*
- ⁷¹ *Physics and Micro Electronic College, Hunan University, Changsha City, China, associated to ⁷*
- ⁷² *Guangdong Provincial Key Laboratory of Nuclear Science, Guangdong-Hong Kong Joint Laboratory of Quantum Matter, Institute of Quantum Matter, South China Normal University, Guangzhou, China, associated to ³*
- ⁷³ *School of Physics and Technology, Wuhan University, Wuhan, China, associated to ³*
- ⁷⁴ *Departamento de Física, Universidad Nacional de Colombia, Bogota, Colombia, associated to ¹³*
- ⁷⁵ *Universität Bonn - Helmholtz-Institut für Strahlen und Kernphysik, Bonn, Germany, associated to ¹⁷*
- ⁷⁶ *Eotvos Lorand University, Budapest, Hungary, associated to ⁴⁸*
- ⁷⁷ *INFN Sezione di Perugia, Perugia, Italy, associated to ²¹*

- ⁷⁸ *Van Swinderen Institute, University of Groningen, Groningen, Netherlands, associated to* ³²
⁷⁹ *Universiteit Maastricht, Maastricht, Netherlands, associated to* ³²
⁸⁰ *National Research Centre Kurchatov Institute, Moscow, Russia, associated to* ⁴¹
⁸¹ *National Research University Higher School of Economics, Moscow, Russia, associated to* ⁴²
⁸² *National University of Science and Technology "MISIS", Moscow, Russia, associated to* ⁴¹
⁸³ *National Research Tomsk Polytechnic University, Tomsk, Russia, associated to* ⁴¹
⁸⁴ *DS4DS, La Salle, Universitat Ramon Llull, Barcelona, Spain, associated to* ⁴⁵
⁸⁵ *Department of Physics and Astronomy, Uppsala University, Uppsala, Sweden, associated to* ⁵⁹
⁸⁶ *University of Michigan, Ann Arbor, United States, associated to* ⁶⁸

^a *Universidade Federal do Triângulo Mineiro (UFMT), Uberaba-MG, Brazil*

^b *Hangzhou Institute for Advanced Study, UCAS, Hangzhou, China*

^c *Excellence Cluster ORIGINS, Munich, Germany*

^d *Università di Bari, Bari, Italy*

^e *Università di Bologna, Bologna, Italy*

^f *Università di Cagliari, Cagliari, Italy*

^g *Università di Ferrara, Ferrara, Italy*

^h *Università di Firenze, Firenze, Italy*

ⁱ *Università di Genova, Genova, Italy*

^j *Università degli Studi di Milano, Milano, Italy*

^k *Università di Milano Bicocca, Milano, Italy*

^l *Università di Modena e Reggio Emilia, Modena, Italy*

^m *Università di Padova, Padova, Italy*

ⁿ *Scuola Normale Superiore, Pisa, Italy*

^o *Università di Pisa, Pisa, Italy*

^p *Università della Basilicata, Potenza, Italy*

^q *Università di Roma Tor Vergata, Roma, Italy*

^r *Università di Urbino, Urbino, Italy*

^s *MSU - Iligan Institute of Technology (MSU-IIT), Iligan, Philippines*

^t *P.N. Lebedev Physical Institute, Russian Academy of Science (LPI RAS), Moscow, Russia*

^u *Novosibirsk State University, Novosibirsk, Russia*

[†] *Deceased*